

## RECENT RESULTS FROM LHCb

AGNIESZKA OBLAKOWSKA-MUCHA

AGH University of Science and Technology  
 Faculty of Physics and Applied Computer Science  
 al. Mickiewicza 30, 30-059 Kraków, Poland

*(Received October 8, 2015)*

The LHCb detector is a single-arm forward spectrometer that collects data at the LHC. In this review, a few of recent results in the field of  $b$ -hadron decays performed by the LHCb Collaboration are presented. The analyses use proton–proton collision data corresponding to  $3 \text{ fb}^{-1}$  collected by the LHCb detector during 2011 and 2012 physics runs with the center-of-mass energies of 7 and 8 TeV.

DOI:10.5506/APhysPolB.47.307

**1. Introduction**

The main motivation for the interest in heavy flavour physics comes from the enormous possibilities to constrain the Standard Model. Of a special interest is to find the probability of the up to down quarks transition amplitudes and angles of the unitary triangles (Fig. 1). All these observables are essential to determine the Cabbibo–Kobayashi–Maskawa (CKM) matrix elements and to look for evidences of physics beyond the Standard Model.

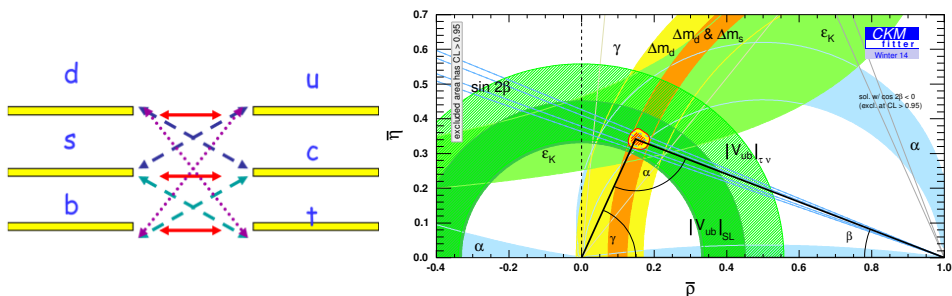


Fig. 1. A schematic representation of transition probabilities among quarks (left). Solid lines correspond to the highest probability, dotted are the least common. The Unitary Triangle with the latest experimental values (right) [1].

The LHCb (Fig. 2) is a dedicated experiment for studying flavour physics at the LHC at CERN. In particular, the experiment is designed to study CP violation and rare beauty and charm particles decays and searches for New Physics evidences. It is a single-arm forward spectrometer covering the pseudorapidity range  $2 < \eta < 5$ . Thus, the LHCb programme is highly complementary to the direct searches performed by the ATLAS and CMS experiments.

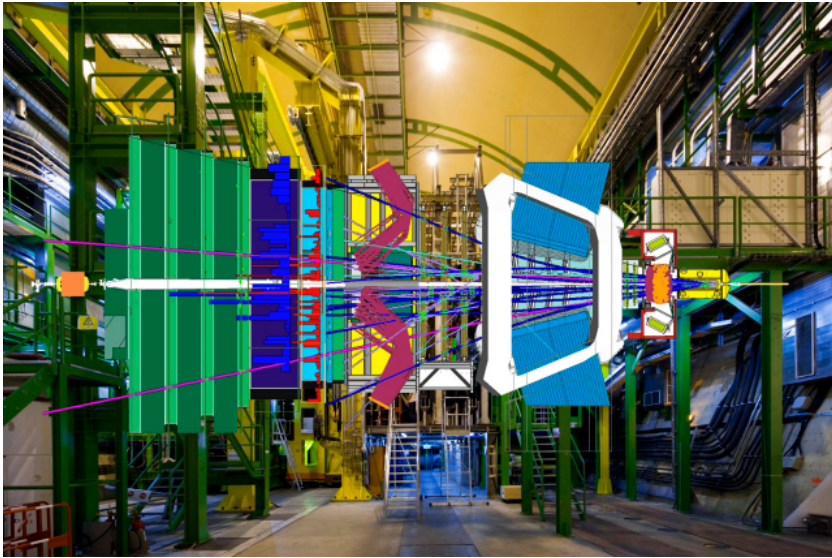


Fig. 2. The LHCb forward spectrometer at the LHC with one of the rare events superposed.

The  $b\bar{b}$ -pairs production in proton–proton collisions is correlated at small angles to the beam axis. The interaction point is surrounded by the Vertex Locator sub-detector, whose role is to precisely determine both the position of the primary vertex and secondary vertices from the decays of beauty and charm particles of the flight distance around 1 cm. In the Run 1 data taking, during the years 2010–12, the LHCb collected  $3 \text{ fb}^{-1}$  of data. The spectrometer achieved an excellent vertex resolution, momentum determination with a precision of  $\delta p/p \sim 0.4\text{--}0.6\%$  and very good particle identification of hadrons in the range of 2–100 GeV. A complete description of the LHCb may be found in Ref. [2].

## 2. Selected results

During Run 1 data taking, the LHCb achieved experimental precision that often matched theoretical predictions. In this review, a few selected results are presented, chosen mainly because of their importance in the field of New Physics or setting new precision limits and discoveries.

### 2.1. Weak phase $\varphi_s$

The  $\varphi_s$  phase comes from the interference between the  $B_s^0$  meson decaying directly to  $J/\psi K^+ K^-$  and the one that is preceded by  $\bar{B}_s^0 - B_s^0$  oscillation. The  $K^+ K^-$  final state goes mainly via  $\phi(1020)$  meson and is in P-wave configuration. So the observed decay final state is a mixture of CP-even and CP-odd components depending on the relative orbital momentum of the  $J/\psi$  and  $\phi$  meson. Theoretically, the decay is decomposed into four time-dependent complex amplitudes. In the measurement, this is implemented by an analysis of the distribution of the reconstructed decay angles of the final state particles in the helicity basis:  $\cos\theta_K$ ,  $\cos\theta_\mu$  and  $\varphi_h$ .

The presented results correspond to the whole sample of  $3 \text{ fb}^{-1}$ . Decay time of selected  $B_s^0$  candidate and the angular distributions fitted with a four components contribution are shown in figure 3.

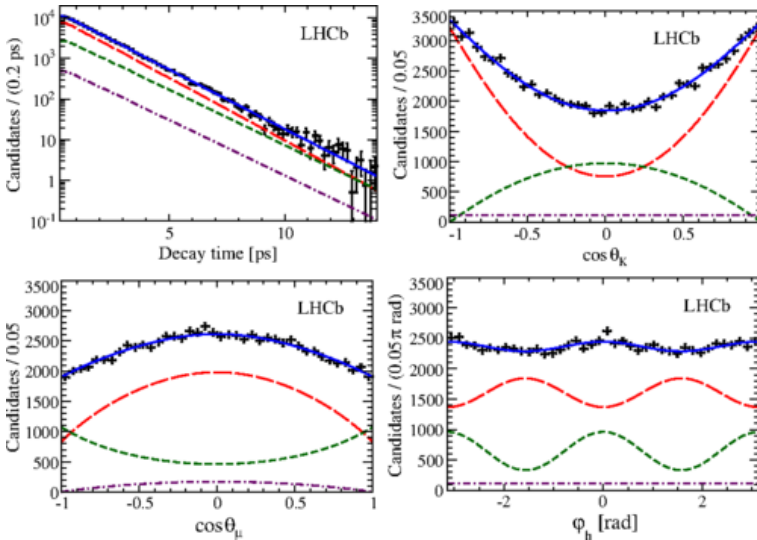


Fig. 3. The decay time of selected  $B_s^0$  candidates (top left). The helicity-angle distribution for the signal events (data points) and total fit (solid/blue line), which is composed with CP-even (long-dashed/red), CP-odd (short-dashed/green) and S-wave (dot-dashed/purple) contribution.

## 2.2. CKM $\gamma$ angle

The CKM  $\gamma$  angle is still the least accurate measured parameter of the unitary triangle. Paradoxically, the theoretical predictions are extremely clean since it can be determined with a pure tree-diagram processes only. Its value may fix the apex of the triangle and finally constrain the Standard Model as a three generation quark scheme. The  $\gamma$  angle is defined as:  $\gamma \equiv \arg\left(-\frac{V_{ud}V_{ub}^*}{V_{cd}V_{cb}^*}\right)$ , so it appears in the interference of  $b \rightarrow c$  and  $b \rightarrow u$  quarks transition.

There are a lot of processes that are sensitive to CKM  $\gamma$  angle, among them are both those which can be performed by time integrated measurement and time-dependent analysis as well. In this review, results coming from the processes of the type  $B \rightarrow DK$  are presented, *i.e.*:  $B^{0(+)} \rightarrow D^0 K^{*(+)}$  and  $B_s^0 \rightarrow D_s^\pm K^\mp$ . These channels have been used for the  $\gamma$  determination for the first time [4, 5].

The CKM  $\gamma$ -angle sensitivity of the  $B^{0(+)} \rightarrow D^0(hh)K^{*(+)}$  channels is much dependent on the ratios of the suppressed to favoured amplitudes ( $r_B, r_D$ ) and strong phases in both  $B$  and  $D$  meson case. The precision of the current results does not allow for the calculation of all these parameters separately, although for the obtained value of  $r_B = 0.240_{-0.048}^{+0.055}$ , the best fit of the  $\gamma$  angle is shown in figure 4.

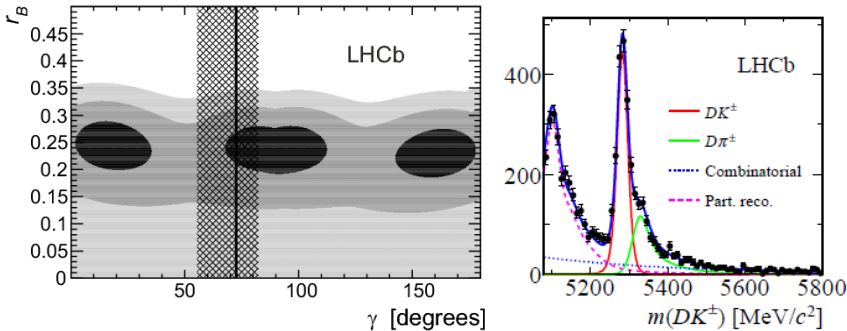


Fig. 4. Plot of two-dimensional fit in  $r_B$  and  $\gamma$  space (left). Line and hashed band correspond to best fit of  $\gamma$  angle and the 68.3% confidence level. Invariant mass distribution of the system  $D^0(K_s^0 K^- K^-)K^+$  (right). Various types of background contribution to the global fit are described in the plot.

For the measurement of the  $\gamma$  angle in  $B^+ \rightarrow D^0(K_s^0 h^+ h^-)K^+$ , a binned Dalitz analysis is performed [5]. In this method, the sensitivity to  $\gamma$  angle is obtained by comparing the distribution of the events in the  $D \rightarrow K_s^0 h^- h^-$  for reconstructed  $B^+$  and  $B^-$  meson. These measurements lead to the value of  $\gamma = (62_{-14}^{+15})^\circ$  what is the most precise result to date obtained with a single method.

In the case of  $B_s^0 \rightarrow D_s^\pm K^\mp$ , a time-dependent analysis is performed what leads to much more experimental difficulties. The obtained value for the CKM  $\gamma$  is:  $\gamma = 115_{-43}^{+28}$  and includes  $1 \text{ fb}^{-1}$  of collected data [6]. It is clear that this very sophisticated method requires not only the whole Run 1 data but data taken during Run 2 as well.

### 2.3. $B_s^0 \rightarrow \mu\mu$ decay

This decay has been searched for the last 30 years. This is a very rare decay that in the Standard Model can proceed via a box diagram only.

The loop diagram with a  $t$  quark and  $W$  boson exchanged is strongly suppressed and  $Z$  exchange is forbidden. The decay  $B^0 \rightarrow \mu\mu$  is even more suppressed due to the transition from third to first quark generation. The significance of the  $B_s^0 \rightarrow \mu\mu$  observation is almost  $6\sigma$ . The combined result is the first clear observation of this decay and leads to the value of the branching ratio:  $\text{BR}(B_s \rightarrow \mu\mu) = 2.8_{-0.6}^{+0.7} \times 10^{-9}$  and  $\text{BR}(B \rightarrow \mu\mu) = 3.9_{-1.4}^{+1.6} \times 10^{-10}$  [7]. Any significant deviation from the Standard Model predictions might give a hint on the SM extension. Two LHC experiments (LHCb and CMS) combined the results and performed a common fit. The mass distribution is presented in figure 5. Both results are statistically compatible with the Standard Model predictions which yields:  $\text{BR}(B_s \rightarrow \mu\mu) = (3.66 \pm 0.23) \times 10^{-9}$  and  $\text{BR}(B \rightarrow \mu\mu) = (1.06 \pm 0.09) \times 10^{-10}$ . These results put stringent constraints on theories beyond the SM.

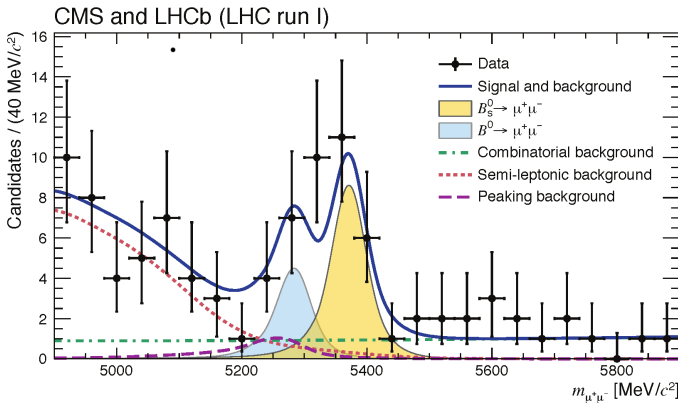


Fig. 5. Dimuon invariant mass distribution. Plot includes data from both experiments obtained by their own selection criteria and combined fit.

### 2.4. Exotic mesons

In the frame of Gell-Mann theory, not only  $|q\bar{q}\rangle$  and  $|qqq\rangle$  objects were proposed, but multiquarks states as well. Such “exotic” hadrons have structures that are more complex and depending on the dominating component can be classified as quarkonia, hybrids, glueballs, dibarions, tetra-quarks (diquark–antidiquarks). There is a lot of predictions in both the charm and beauty sector for the existence of tetraquark states. In this review, the latest study of two of them:  $X(3872)$  and  $Z(4430)^-$  is presented.

The  $X(3872)$  was previously seen in other experiments and neither its charmonium origin nor an interpretation as an exotic state: tetraquark  $c\bar{c}c\bar{u}$  or molecule  $D^0D^0 = (c\bar{u})(\bar{c}u)$  were excluded. The LHCb has shown this state produced in the process  $B^+ \rightarrow X(3872)K^+$  decaying into charmonium state:  $X(3872) \rightarrow J/\psi\pi^+\pi^-$ . The full angular analysis in helicity basis was performed in order to determine its quantum numbers. The hypothesis of  $J^{PC} = 1^{++}$  is the one that is unambiguously preferred by the data, see Fig. 6. This result favours exotic explanations of the  $X(3872)$  state and excludes charmonium, but cannot settle whereas it is a tetraquark or molecule.

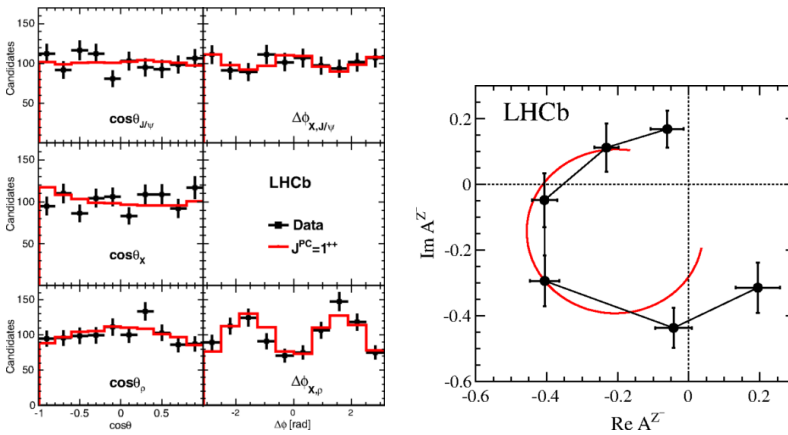


Fig. 6. Distribution of the helicity angles of the background-subtracted events  $X(3872) \rightarrow J/\psi\pi^+\pi^-$  with a fit for  $1^{++}$  hypothesis (left). The Argand diagram of the  $\psi'\pi^-$  signal  $Z(4430)^-$  events (right).

Much more controversy aroused around another exotic candidate — the charged  $Z(4430)^-$ . Taking advantage of a huge statistic of events, the LHCb observed this exotic object in the process  $B^0 \rightarrow \psi'K^+\pi^-$ , where  $Z(4430)^- \rightarrow \psi'\pi$ . This is a state with a quark content  $c\bar{c}d\bar{u}$  and might be the first observation of the meson beyond  $q\bar{q}$  model.

The main achievements in this study is the determination of the quantum numbers of this state and proving that it has a resonant origin. A 4-D model-dependent amplitude fit with all known  $K^{*0} \rightarrow K^+\pi^-$  resonances was performed. The data are well described with a spin  $1^+$ , where the positive parity favours four-quark bound state as the only plausible explanation. In addition, the Argand diagram obtained for  $Z(4430)^-$  amplitude (see Fig. 6) is consistent with its resonant behaviour. The measured mass is  $4475 \pm 7^{+15}_{-3.3}$  MeV and width:  $172 \pm 13^{+37}_{-34}$  MeV [9].

A further searches in this field are ongoing, amongst the most interesting one is just recently done observation of pentaquark-like state in  $\Lambda_b^0 \rightarrow J/\psi p K^-$  decays [10].

### 3. Summary

The LHCb spectrometer features outstanding tracking and vertexing performance and has already demonstrated high ability to accomplish the precise results in heavy flavour sector. The CKM  $\gamma$  angle was determined with the best precision and with new methods. The search of New Physics has not showed unambiguous evidences. Both the weak phase  $\phi_s$  and branching fractions of the  $B_{(s)} \rightarrow \mu\mu$  decays are within the Standard Model limits. The laborious analysis oriented on multiquarks states succeeded in discovering at least two states which show exotic behaviour.

### REFERENCES

- [1] [http://ckmfitter.in2p3.fr/www/html/ckm\\_results.html](http://ckmfitter.in2p3.fr/www/html/ckm_results.html)
- [2] A.A. Alves, Jr. *et al.* [LHCb Collaboration], *JINST* **3**, S08005 (2008).
- [3] R. Aaij *et al.* [LHCb Collaboration], *Phys. Rev. Lett.* **114**, 041801 (2015).
- [4] R. Aaij *et al.* [LHCb Collaboration], *Phys. Rev. D* **90**, 112002 (2014).
- [5] R. Aaij *et al.* [LHCb Collaboration], *J. High Energy Phys.* **1410**, 097 (2014).
- [6] R. Aaij *et al.* [LHCb Collaboration], *J. High Energy Phys.* **1411**, 060 (2014).
- [7] V. Khachatryan *et al.* [CMS and LHCb collaborations], *Nature* **522**, 68 (2015).
- [8] R. Aaij *et al.* [LHCb Collaboration], *Phys. Rev. Lett.* **110**, 222001 (2013).
- [9] R. Aaij *et al.* [LHCb Collaboration], *Phys. Rev. Lett.* **112**, 222002 (2014).
- [10] R. Aaij *et al.* [LHCb Collaboration], *Phys. Rev. Lett.* **115**, 072001 (2015).